

Selection of intensity measures for displacement prediction of geosynthetic reinforced soil walls under seismic loading

Cihan Cengiz^{1*}, Ismail Emrah Kilic², and Erol Guler³

¹Deltares, Boussinesqweg 1, 2629 HV Delft, the Netherlands

²Royal HaskoningDHV, 3818 EX Amersfoort, the Netherlands

³George Mason University, 4400 University Dr, Fairfax, VA 22030, USA

Abstract. The accurate prediction of damage in Geosynthetic Reinforced Soil (GRS) walls is critical for the safe and cost-effective design of infrastructure systems, particularly in seismic or extreme loading environments. This paper investigates the selection of appropriate Intensity Measures (IMs) for predicting damage to GRS walls under various loading scenarios. A comprehensive analysis is conducted, comparing different IMs based on their correlation with wall performance indicators, including displacement, reinforcement strain, and facing deformations. The study explores the suitability of IMs such as peak ground acceleration (PGA), spectral acceleration, and Arias intensity, focusing on their ability to provide reliable predictions of wall damage under dynamic conditions. Numerical simulations are employed to model the behavior of GRS walls under seismic loads, and empirical data from previous tests is used to validate the results. The findings suggest that certain IMs, particularly those capturing energy dissipation and frequency content, offer enhanced predictive capability compared to traditional measures. This research provides valuable insights into the selection of IMs for improving the design and resilience of GRS walls, with implications for both the seismic and geotechnical engineering communities.

1 Introduction

Geosynthetic Reinforced Soil Walls (GRS Walls) are widely used as a part of the civil infrastructure world-wide. Their use has seen increasing demand due to their cost effectiveness, reasonable ease of building, and robust design which can withstand various loading conditions. Specifically, GRS walls are reported to exhibit good performance against seismic loads as evidenced by many large earthquakes [1-5]. GRS walls are also observed to outperform conventional retaining walls [4] which was exemplified through many GRS

* Corresponding author: cihan.cengiz@deltares.nl

structures remaining in service after major earthquakes while conventional structures have not [6]. Due to the exceptional seismic performance of GRS walls, these structures have been implemented as a means to support critical infrastructure such as high-speed rail networks in areas with high seismic demands like Japan [3].

There is a very wide body of research on the seismic behavior of GRS walls with a multitude of works involving physical and numerical modelling. There have been numerous pioneering studies which have modelled the GRS walls through 1-g shaking table tests [7, 8] and additionally n-g centrifuge tests [9, 10]. Similarly, there have been numerous studies on the numerical analysis of GRS walls [11-13]. Despite the well-established research body on the seismic response of GRS walls, there is a lack of studies on the damage prediction of these structures which can improve the resilience of these critical infrastructure assets.

In seismically induced damage prediction of Geosynthetic Reinforced Soil (GRS) walls, the selection and subsequent use of Intensity Measures (IMs) can substantially enhance the state of engineering design as IMs provide a direct link between ground motion characteristics and structural response. Although there are limited studies elaborating these links, some researchers have reported on this connection. For example, the Arias Intensity has been shown to correlate well with the reinforcement strains and facing displacements [14, 15] of GRS walls. Despite these efforts, there are no studies exploring how different intensity measures correlate with the structural response. Studies probing in this direction have the potential to improve upon the traditional approaches, such as deterministic design methods or simplified pseudo-static analyses which often cannot capture the complexities of seismic response of GRS walls.

This contribution aims to showcase an exemplar case where IMs could be used to estimate damage and to improve the resilience of GRS walls. To that end, a numerical model utilizing a 2D plane strain model was created in a commercially available software and time-history analyses were run utilizing various input motions consistent with the Incremental Dynamic Analysis procedure outlined by Vamvatsikos and Cornell [16]. The results demonstrate the predictive powers of various IMs in determining the damage potential of the GRS walls. It is noted here that the seismic fragility assessment of the studied GRS system is outside of the scope of the present study. Lastly, a direct comparison with unreinforced configurations was not included in this study, as the beneficial role of reinforcement is already well established in the literature and forms the basis of this work.

2 Selected Input Motions and Intensity Measures

2.1 Input Motions

The input motions selection follows the procedure outlined by Karafagka et al [17] where 15 strong-motion records were retrieved from the European Strong Motion Database. This large number of signals was selected to have a statistically meaningful outcome of the conducted analysis. The motions outlined in Table 1 are taken from sites with ground types A and B according to the classification outlined in Eurocode 8 (EC8) [18]. The selection of the ground motions was optimized with the REXEL software to be compatible with the reference spectrum proposed by Akkar and Bommer [19]. This reference spectrum is based on the ground-motion prediction equations (GMPEs) developed by the aforementioned authors [19]. These models were derived from an extensive European and Middle Eastern strong-motion database, comprising 532 accelerograms recorded from 131 earthquakes with moment magnitudes ranging from Mw 5.0 to 7.6 and source-to-site distances up to 100 km. The spectrum predicts 5%-damped pseudo-spectral accelerations (PSA), using a functional

form that accounts for magnitude scaling, distance attenuation, fault mechanism, and site effects, with separate coefficients for intra-event and inter-event variability.

Fig. 1 illustrates the comparison between the spectrum prescribed by Akkar and Bommer (2010) and the elastic response spectra of the selected motions. Fig. 1 also provides a more detailed and transparent view of the selected motions by showing the normalized spectra for all motions and their mean, and also illustrates how these spectra compare to those of Akkar and Bommer (2010).

Table 1. Selected input motions and their properties.

Earthquake Name	Date	Mw	Fault mechanism	Epicentral distance (km)	PGA (m/s ²)	EC8 Site Class	ID*	Horz. Comp.**
Umbria Marche (aftershock)	06-10-1997	5.5	Normal	5	1.838	A	651	y
Valnerina	19-09-1979	5.8	Normal	5	1.51	A	242	x
SE of Tirana	09-01-1988	5.9	Thrust	7	4.037	A	3802	y
Lazio Abruzzo (aftershock)	11-05-1984	5.5	Normal	15	1.411	A	990	x
Valnerina	19-09-1979	5.8	Normal	5	2.012	A	242	y
Kozani	13-05-1995	6.5	Normal	17	2.039	A	6115	x
Friuli (aftershock)	15-09-1976	6.0	Thrust	12	1.339	A	149	x
Umbria Marche	26-09-1997	5.7	Normal	23	1.645	A	763	y
Friuli (aftershock) Patras	15-09-1976	6.0	Thrust	14	2.586	B	134	x
Patras	14-07-1993	5.6	Strike-slip	9	3.337	B	1932	y
Kalamata	13-09-1986	5.9	Normal	11	2.67	B	414	y
Umbria Marche 2	26-09-1997	6.0	Normal	11	5.138	B	594	x
Montenegro (aftershock)	24-05-1979	6.2	Thrust	17	1.708	B	229	x
Kefallinia island	23-01-1992	5.6	Thrust	14	2.223	B	6040	y
Ano Liosia	07-09-1999	6.0	Normal	14	2.159	B	1714	y

*The identification number of the input motion in the European Strong Motion Database

**Horizontal component of the selected motion

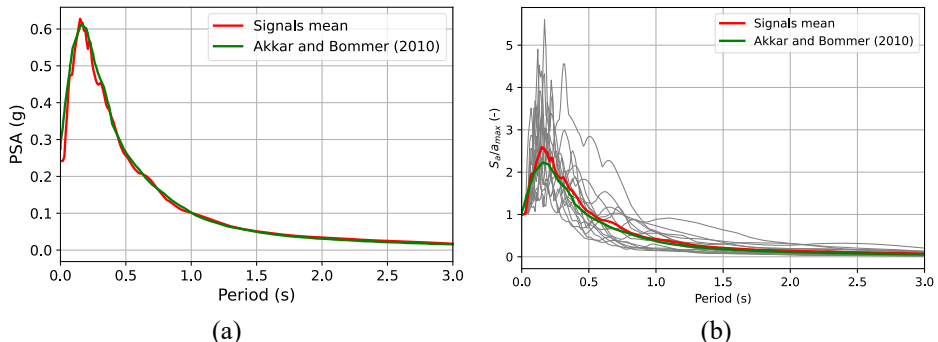


Fig. 1. (a) Comparison of the mean elastic response spectrum of the selected motions with the reference spectrum proposed by Akkar and Bommer (2010) [19]; (b) normalized elastic response spectra of all selected motions shown in grey curves, their mean spectrum, and the reference spectrum proposed by Akkar and Bommer (2010) [19].

2.2 Intensity Measures

Although a large number of intensity measures have been reported in the literature [20], within the scope of this study a limited number of intensity measures are considered. These intensity measures are listed below:

- PGA: While there are historic reasons such as its availability in as to why Peak Ground Acceleration (PGA) is commonly used as an intensity measure, many works in the literature investigating the predictive powers of different IMs have concluded that this parameter is not a very good estimator of damage [21]. Beyond historical reasons, PGA is a parameter that is used in assessment of seismic hazard, ground motion prediction equations, liquefaction susceptibility calculations, and its utility in being applied as a direct parameter for pseudo-static analysis where it is used as a coefficient for horizontal loading. Therefore, for completeness, this parameter is often included as an IM. It must be noted that there are exceptional cases where PGA is regarded as a good estimator of damage [22] but overwhelming majority of findings in the literature suggest otherwise.
- Peak Ground Velocity (PGV) is another widely recognized intensity measure in predicting structural and geotechnical damage. It is particularly preferred for flexible systems.
- Peak Ground Displacement (PGD) is a relevant parameter for understanding seismic displacement demands in (long-period) infrastructure assets such as bridges, pipelines, and retaining walls.
- Cumulative Absolute Velocity (CAV) measures the cumulative effects of the strong motion and unlike the parameters listed above, it also accounts for the duration of the event [23]. This parameter is widely recognized as a good estimator of damage. CAV is expressed in the following manner:

$$CAV = \int_0^{t_{max}} |a(t)| dt \quad (1)$$

- Arias Intensity, (IA) [24] is a measure of the cumulative seismic energy given by an earthquake. This parameter has been shown to predict the seismic settlement of structures in general [25] and geosynthetic reinforced soil bodies follow the pattern of IA curve [26]. It is also known that IA correlates well with several commonly used demand measures of structural performance, liquefaction, and seismic slope stability [26]. IA is expressed in the following form:

$$IA = \frac{\pi}{2g} \int_0^{T_d} a(t)^2 dt \quad (2)$$

- Shaking Intensity Rate (SIR) is a seismic intensity measure that takes the rate of seismic energy build up into account and it normalizes the IA_{5-75} is the change in IA from 5 to 75% of its total value, and D_{5-75} is the corresponding time duration (see below for the formulation).

$$SIR = \frac{IA_{5-75}}{D_{5-75}} \quad (3)$$

3 Analysis Procedure

3.1 Incremental Dynamic Analysis

In the beginning of 2000s, Vamvatsikos and Cornell [16] defined the Incremental Dynamic Analysis (IDA) procedure to evaluate the seismic performance of structures. Since its inception, the method has found widespread use in civil and geotechnical engineering circles. The analysis method involves incrementally scaling the selected set of ground motions to capture both the elastic and plastic response of the infrastructure asset in question. By applying input motions of successively increasing intensity, the structural response is monitored by employing an engineering demand parameter such as settlement (for example for embankments) or story drift (for multi-storey structures). The intensity scaling is generally done with linearly scaling the Peak Ground Acceleration (PGA) of the motion. The IDA procedure can also be used to estimate the probability of exceeding various damage states which aids in defining fragility functions. This is especially robust in cases where damage states are clearly defined as in the case of transport embankments. An excellent example of such a study on seismic fragility of transport embankments is presented by Argyroudis and Kaynia [27] where the damage state selection for highways and railways involved a rigorous investigation. While well-established damage states are available for some infrastructure assets, to the knowledge of the authors, no universally agreed upon guideline exists for GRS walls.

3.2 Analysed GRS Wall and Numerical Modelling

The analysed GRS wall is 6.0 m high with reinforcement length $L/H = 0.75$ (4.5 m) and vertical spacing of 60 cm. Geogrid reinforcements have axial stiffness $EA = 1500$ kN/m. Facing blocks are modelled as 0.20 m thick concrete panels with stiffness 4.5×10^6 kN/m, Poisson's ratio 0.1, and unit weight 3.6 kN/m²/m.

The backfill, modelled as dense sand with HSsmall, has $\phi = 35^\circ$, $c = 1$ kPa, $\gamma = 19$ kN/m³, $E_{oed,ref} = 50,000$ kPa, $E_{50,ref} = 60,000$ kPa, $E_{ur,ref} = 180,000$ kPa, $\nu = 0.3$, $G_0 = 120,000$ kPa, and $G_s = 0.722 G_0$ at $\gamma = 0.0001$.

Foundation soil (Eurocode 8, type B) is also HSsmall, with $V_s = 600$ m/s, $\gamma = 20$ kN/m³, $\phi = 32^\circ$, $c = 5$ kPa, $E_{oed,ref} = 80,000$ kPa, $E_{50,ref} = 100,000$ kPa, $E_{ur,ref} = 300,000$ kPa, $\nu = 0.35$, $G_0 = 180,000$ kPa, and $G_s = 0.722 G_0$ at $\gamma = 0.0002$.

3.3 Characteristics of an Optimal Intensity Measure

Padgett et al [22] prescribes a set of criteria (or statistical parameters) to select optimal intensity measures. Within the context of the forthcoming study, three of these will be investigated. These parameters are the following:

- Efficiency: This parameter shows the dispersion of the damage around the mean of the results, and it is expressed in the following manner:

$$\beta_{D|IM} = \sqrt{\frac{\sum (\ln(d_i) - \ln(aIM^b))^2}{N - 2}} \quad (4)$$

- Practicality: In simplest terms, this parameter relates to the slope of the IM versus damage trend. This is explained in a pictorial form in Fig. 2

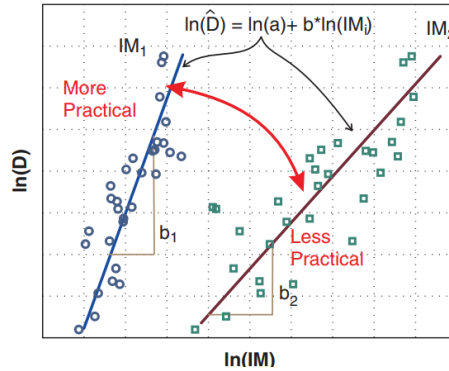


Fig. 2. An exemplar representation of relative practicality of intensity measures [22] where scatter plots of different intensity measures are shown to have varying slopes.

- Proficiency: This metric is a composite measure of the efficiency and practicality parameters introduced above.

$$\zeta = \frac{\beta_{D|IM}}{b} \tag{5}$$

where $\beta_{D|IM}$ is the efficiency and b is the slope of the intensity measure versus damage state line.

4 Results

The results are compared taking the displacements of the top corner of the GRS wall. The vertical and horizontal displacements are evaluated separately. Fig. 3 illustrates the plots considered intensity measures versus the vertical settlement of the topmost corner of the GRS wall. These plots illustrate the spread of the data as well as the coefficient of determination pertaining to each intensity measure. The coefficient of determination in each plot indicates that parameters such as PGA and its derivatives do not provide a good set of data to predict the damage in general. However, parameters considering the cumulative and duration effects of the earthquake give a better representation of the damage potential. For example, the coefficient of determination for IA is about 0.91 and the value for SIR is a close second at about 0.90. A similar trend is observed in Fig. 4 where the lateral deformation of the GRS wall is considered. In both figures, it is observed that the coefficients of determination for IA and SIR are the highest.

Beyond the coefficient of determination, the above prescribed intensity measure metrics, namely, efficiency, practicality, and proficiency also shed light on the selection of the optimum intensity measure for damage prediction of the GRS wall considered herein. Table 2 gives an account on the outcomes of the parameters introduced by Padgett et al [22] where the performance of different IMs in predicting the wall deformations are illustrated. According to efficiency metric, the most suitable intensity measure is IA for estimating both the settlement and the lateral deformation of the wall. IA is followed by SIR. In terms of practicality however, due to the large spread in the parameter, IA exhibited a milder slope than that of its counterparts. In this regard, SIR slightly outperformed IA. In the overall comparison of the metrics, in terms of proficiency, IA ranks highest as it balances low dispersion with acceptable practicality. Beyond the coefficient of determination, Table 2 shows that while PGV has the highest proficiency for settlement alone, it underperforms for lateral deformation. In contrast, IA consistently shows low dispersion (highest efficiency) and competitive proficiency across both damage metrics. Considering the overall balance of

performance rather than individual metrics in isolation, IA emerges as the most robust predictor in this study.

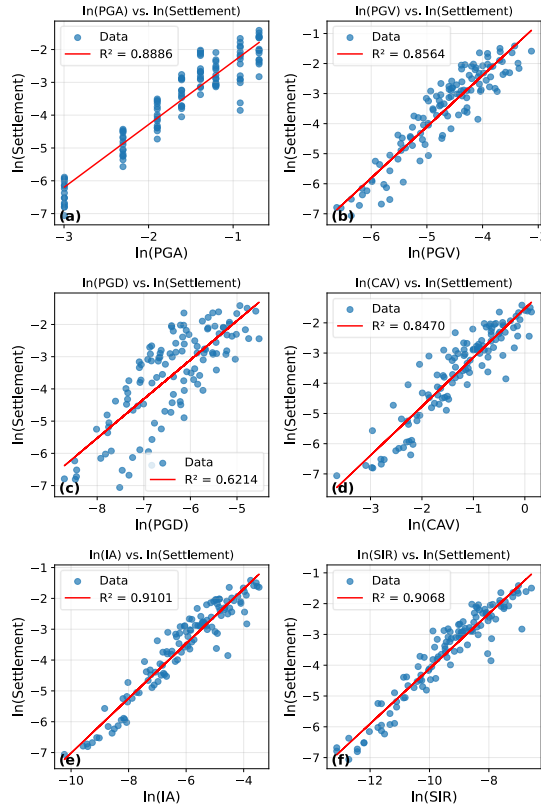


Fig. 3. Plots of natural logarithm of settlement natural logarithm of settlement and different IMs.

Table 2. Performance metrics (Efficiency, Practicality, and Proficiency) of various seismic Intensity Measures (IMs) in predicting Settlement and Lateral Deformation.

IM	Settlement			Lateral Deformation		
	Efficiency	Practicality	Proficiency	Efficiency	Practicality	Proficiency
PGA	0.484	1.915	0.253	0.505	1.467	0.345
PGV	0.550	1.708	0.322	0.490	1.342	0.365
PGD	0.893	1.214	0.735	0.726	0.966	0.752
CAV	0.568	1.620	0.350	0.472	1.291	0.366
IA	0.435	0.888	0.490	0.388	0.703	0.552
SIR	0.443	0.894	0.496	0.396	0.708	0.559

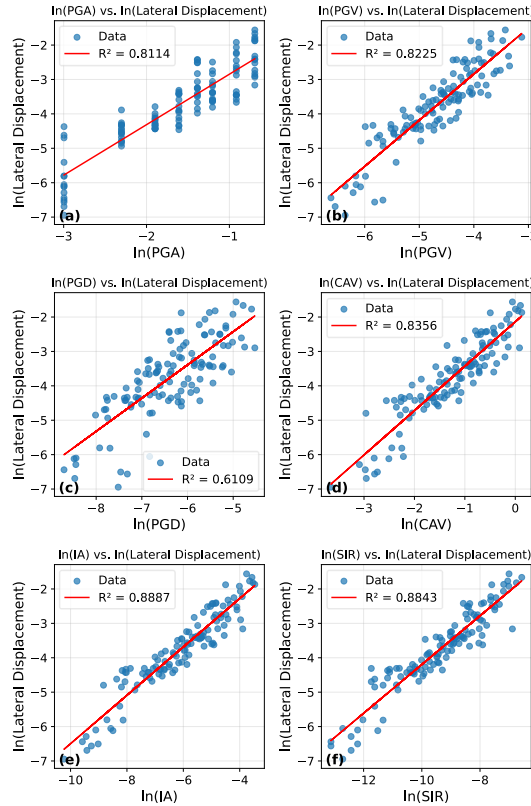


Fig. 4. Plots of natural logarithm of maximum facing displacement versus natural logarithm of settlement and different IMs.

The comparison of settlement and lateral deformation trends indicates that cumulative IMs exhibit better predictive capabilities and performance across both damage metrics. In contrast, traditional IMs such as PGA show variability and often fail to account for the intricacies of the seismic responses in GRS walls. This finding shows the importance of adopting advanced IMs (incorporating many aspects of the seismic input such as the imparted energy, duration, and frequency content) in seismic design considerations.

5 Conclusions

This study investigated the selection of appropriate Intensity Measures (IMs) for predicting the seismically induced damage in Geosynthetic Reinforced Soil (GRS) walls. A model wall typology was subjected to increasing amplitude of input motions through the procedure known as Incremental Dynamic Analysis. As a result of the dynamic time-history analysis, the structural damage (settlement of the topmost elevation of the wall and maximum facing displacements) was correlated with the intensity measures. The intensity measures investigated were, PGA, PGV, PGD, CAV, IA and SIR. As a result of the conducted analysis following conclusions can be specified:

- Arias Intensity (IA) and Shaking Intensity Rate (SIR) were identified as the most effective IMs for predicting both settlement and lateral deformation. This was substantiated based on the high coefficient of determination yielded by both of these parameters and the relatively low dispersion in the results. Conventional

intensity measures such as PGA and its derivatives performed poorly in this regard. It is once again shown that intensity measures which can capture both the cumulative energy input, duration, and other complex aspects of the strong motion are better suited to predict damage.

- There are emerging works which can estimate the IA of an expected earthquake at a given site based on the proximity to the fault, dominant faulting mechanism, path effects, and other parameters. Seismic design can leverage these to come up with robust designs of infrastructure assets.
- Future studies should incorporate a wider range of wall typologies and a larger selection of intensity measures. Currently available literature possesses in the order of 30-40 promising candidates.

References

1. J. Collin, V. Chouery-Curtis, and R. Berg, Field observations of reinforced soil structures under seismic loading. in International symposium on earth reinforcement practice (1992)
2. D. Sandri, A performance summary of reinforced soil structures in the greater Los Angeles area after the Northridge earthquake. *Geotext. Geomembr.* **15**(4-6), 235-253 (1997) [https://doi.org/10.1016/S0266-1144\(97\)10006-1](https://doi.org/10.1016/S0266-1144(97)10006-1)
3. F. Tatsuoka, Performance of reinforced soil structures during the 1995 Hyogo-ken Nambu Earthquake, Special Lecture. in Int. Symp. Earth Reinforcement, IS Kyushu'96 Balkema (1997)
4. H.I. Ling, D. Leshchinsky, and N.N. Chou, Post-earthquake investigation on several geosynthetic-reinforced soil retaining walls and slopes during the Ji-Ji earthquake of Taiwan. *Soil. Dyn. Earthquake. Eng.* **21**(4), 297-313 (2001) [https://doi.org/10.1016/S0267-7261\(01\)00011-2](https://doi.org/10.1016/S0267-7261(01)00011-2)
5. R. Race, and H. Del Cid, Seismic performance of modular block retaining wall structures during the January 2001 El Salvador earthquake. in Proc., Int. Geosynthetic Engineering Forum 2001, (2001)
6. J. Koseki et al, Seismic stability of reinforced soil walls. in 8th international conference on Geosynthetics (2006)
7. R. Bathurst and K. Hatami, Seismic response analysis of a geosynthetic-reinforced soil retaining wall. *Geosynt. Int.* **5**(1-2), p. 127-166 (1998)
8. H.I. Ling et al., Large-scale shaking table tests on modular-block reinforced soil retaining walls. *J. Geotech. Geoenviron. Eng.* **131**(4), 465-476 (2005) [https://doi.org/10.1061/\(ASCE\)1090-0241\(2005\)131:4\(465\)](https://doi.org/10.1061/(ASCE)1090-0241(2005)131:4(465))
9. J. Takemura, and A. Takahashi, Centrifuge modeling of seismic performance of reinforced earth structures, in Reinforced soil engineering, CRC Press, p. 414-438 (2003)
10. H.I. Ling et al., Analyzing dynamic behavior of geosynthetic-reinforced soil retaining walls. *J. Eng. Mech.* **130**(8), 911-920 (2004) [https://doi.org/10.1061/\(ASCE\)0733-9399\(2004\)130:8\(911\)](https://doi.org/10.1061/(ASCE)0733-9399(2004)130:8(911))
11. Y. Yu, R.J. Bathurst and T.M. Allen, Numerical modeling of the SR-18 geogrid reinforced modular block retaining walls. *J. Geotech. Geoenviron. Eng.* **142**(5): p. 04016003 (2016) [https://doi.org/10.1061/\(ASCE\)GT.1943-5606.0001438](https://doi.org/10.1061/(ASCE)GT.1943-5606.0001438)

12. R. Bathurst and K. Hatami, Review of numerical modeling of geosynthetic reinforced soil walls. in Proc., 10th Int. Conf. on Computer Methods and Advances in Geomechanics. Balkema, Tucson, AZ, USA (2001)
13. E. Guler, M. Hamderi and M. Demirkan, Numerical analysis of reinforced soil-retaining wall structures with cohesive and granular backfills. *Geosynt. Int.* **14**(6): p. 330-345 (2007) <https://doi.org/10.1680/gein.2007.14.6.330>
14. H. Liu, C. Hung and J. Cao, Relationship between Arias intensity and the responses of reinforced soil retaining walls subjected to near-field ground motions. *Soil. Dyn. Earthquake. Eng.* **111**, 160-168 (2018) <https://doi.org/10.1016/j.soildyn.2018.04.022>
15. C. Cengiz, E. Kilic, and E. Guler, On the interplay between seismic input energy and reinforcement strain. in 11th International Conference on Geosynthetics–11 ICG. Seoul, South Korea. 2018.
16. D. Vamvatsikos, and C.A. Cornell, Incremental dynamic analysis. *Earthquake Eng. Struct. Dyn.* **31**(3), 491-514 (2002) <https://doi.org/10.1002/eqe.141>
17. S. Karafagka, et al., Fragility curves of non-ductile RC frame buildings on saturated soils including liquefaction effects and soil–structure interaction. *Bull. Earthquake Eng.* **19**(15), 6443-6468 (2021) <https://doi.org/10.1007/s10518-021-01081-5>
18. European Committee, Eurocode 8: Design of structures for earthquake resistance—Part 5: Foundations, retaining structures, and geotechnical aspects. Brussels, Belgium: European Committee for Standardization (2004)
19. S. Akkar and J.J. Bommer, Empirical equations for the prediction of PGA, PGV, and spectral accelerations in Europe, the Mediterranean region, and the Middle East. *Seismol. Res. Lett.* **81**(2), 195-206 (2010) <https://doi.org/10.1785/gssrl.81.2.195>
20. S. Dashti and Z. Karimi, Ground motion intensity measures to evaluate I: The liquefaction hazard in the vicinity of shallow-founded structures. *Earthquake Spectra* **33**(1), 241-276 (2017) <https://doi.org/10.1193/103015eqs162m>
21. G. Tsinidis et al., Optimal intensity measures for the structural assessment of buried steel natural gas pipelines due to seismically-induced axial compression at geotechnical discontinuities. *Soil. Dyn. Earthquake. Eng.* **131**, 106030 (2020) <https://doi.org/10.1016/j.soildyn.2019.106030>
22. J.E. Padgett, B.G. Nielson and R. DesRoches, Selection of optimal intensity measures in probabilistic seismic demand models of highway bridge portfolios. *Earthquake Eng. Struct. Dyn.* **37**(5), 711-725 (2008) <https://doi.org/10.1002/eqe.782>
23. M.D. Trifunac and A.G. Brady, A study on the duration of strong earthquake ground motion. *Bull Seismol Soc Am* **65**(3), 581-626 (1975) <https://doi.org/10.1785/BSSA0650030581>
24. A. Arias, A measure of earthquake intensity. *Seismic design for nuclear plants.* 438-483 (1970)
25. S. Dashti, et al. Mechanisms of seismically induced settlement of buildings with shallow foundations on liquefiable soil. *J. Geotech. Geoenviron. Eng.* **136**(1), 151-164 (2010) [https://doi.org/10.1061/\(ASCE\)GT.1943-5606.0000179](https://doi.org/10.1061/(ASCE)GT.1943-5606.0000179)
26. C. Cengiz and E. Guler, Load bearing and settlement characteristics of Geosynthetic Encased Columns under seismic loads. *Soil. Dyn. Earthquake. Eng.* **136**, 106244 (2020) <https://doi.org/10.1016/j.soildyn.2020.106244>
27. S. Argyroudis and A.M. Kaynia, Analytical seismic fragility functions for highway and railway embankments and cuts. *Earthquake Eng. Struct. Dyn.* **44**(11), 1863-1879 (2015) <https://doi.org/10.1002/eqe.2563>